Supplementary Figure 1

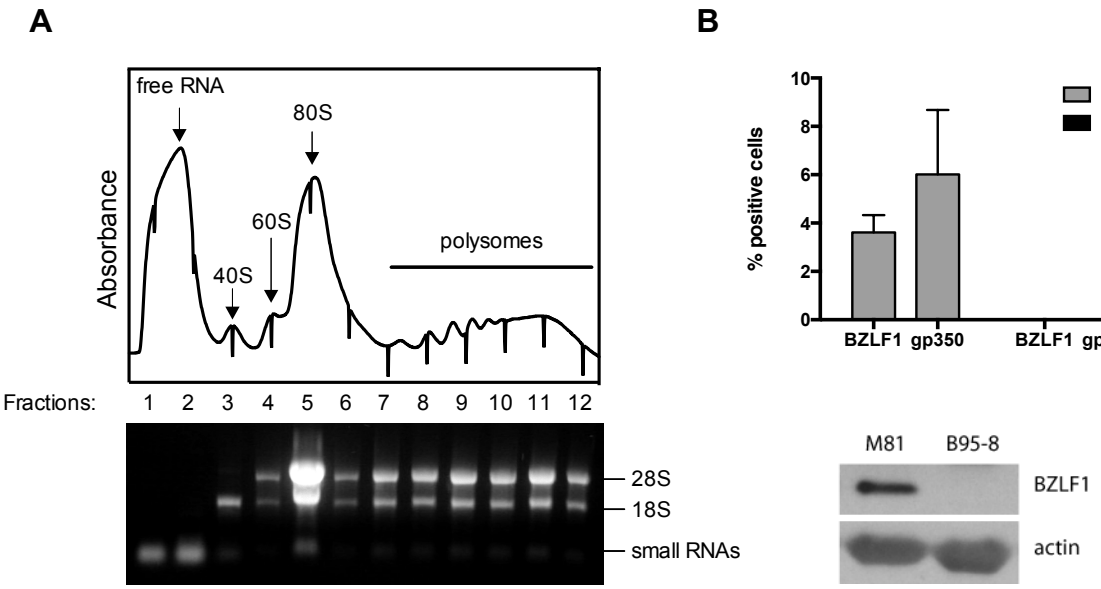

Supplementary Figure 1: Ribosome profiling of EBV-infected LCLs. (**A**) Representative polysome profile obtained after sucrose density centrifugation of RNA-protein complexes extracted from a LCL treated with cycloheximide. The types of RNA-ribosome complexes that were separated by the gradient are depicted below the profile. The RNA species present in the different fractions were purified and loaded onto an agarose gel to visualize the 18S and 28S rRNAs. Fractions 1 and 2 contain free RNA devoid of ribosomes, fraction 3 corresponds to the 40S ribosomal subunit associated with RNA as demonstrated by the presence of 18S rRNA in the absence of 28S RNA, fraction 4 mainly contains 60S ribosomal subunit with a predominance of 28S rRNAs, fractions 5 to 7 contain RNA associated to a single 80S ribosome as shown by the presence of both 18S and 28S rRNAs, whereas fractions 8 to 12 contain RNA bound to an increasing number of polysomes that migrate more and more quickly in the sucrose gradient. (**B**) Lytic replication levels in the samples used for library generation. Immunofluorescence stainings for the lytic cycle proteins revealed the percentage of cells expressing BZLF1 and gp350 in LCLs infected with M81 or B95-8 that is given in the graph of bars. Below we show a representative western blot with a BZLF1-specific antibody using extracts of LCLs infected with either one of the two strains.

Supplementary Figure 2

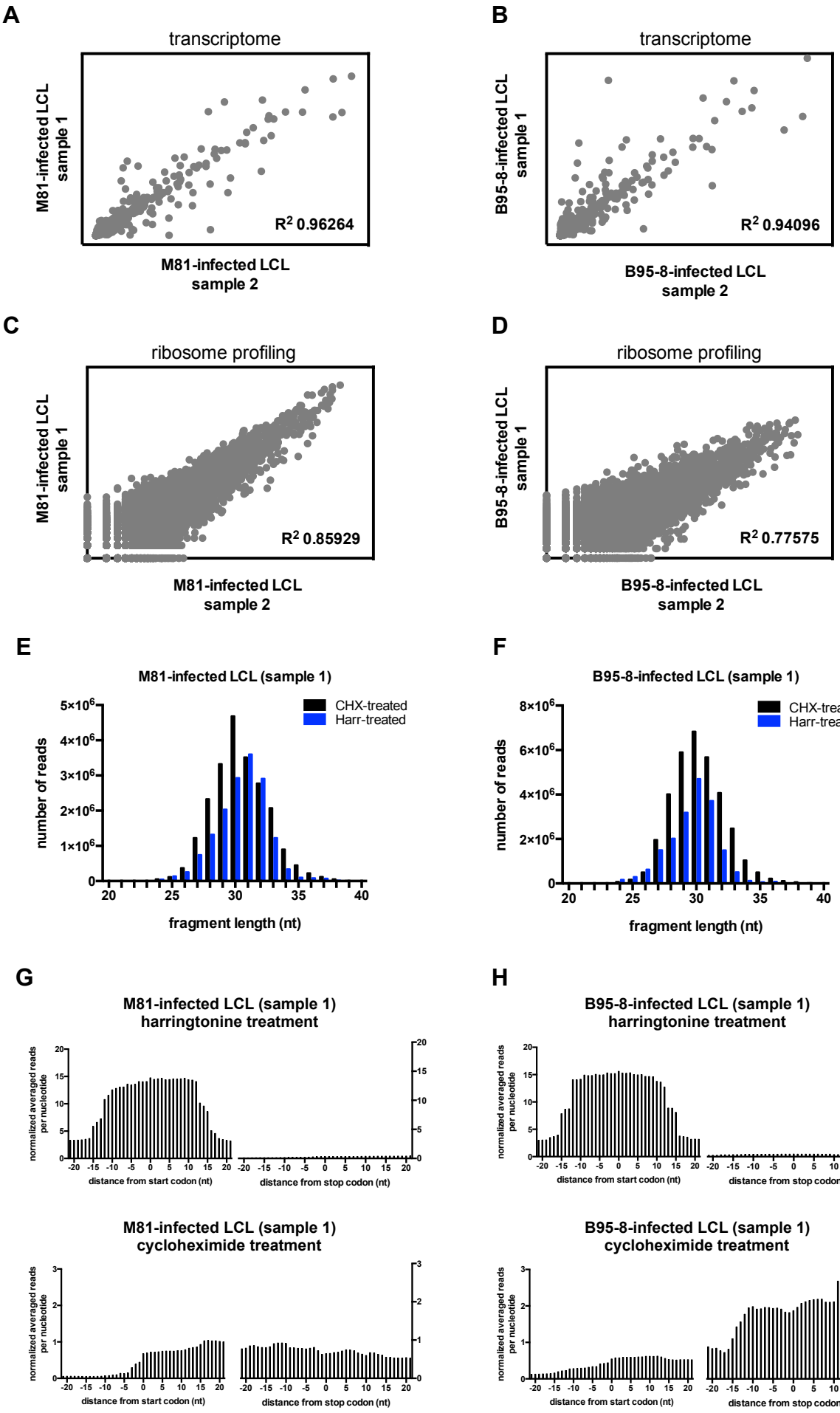

Supplementary Figure 2: Quality control data of the sequencing experiments.

(**A**) For each cellular gene, the reads per kilobase per million mapped reads (RPKM) obtained by total RNA sequencing of the M81-infected LCL generated from sample 1 are plotted against the RPKM values obtained from total RNA sequencing of M81-infected LCLs from sample 2. We indicated the Pearson's correlation coefficient between the two data sets. (**B**) Same as in (**A**) but with RPKM values obtained from total RNA sequencing of B95-8-infected LCLs. (**C**) For each cellular gene, the number of ribosome-protected fragments sequenced from the LCLs generated with sample 1 by infection with M81 and treatment with harringtonine for 2 min was plotted against its counterpart generated with sample 2 and the resulting Pearson correlation coefficient is given. (**D**) Same as in (**C**) but with cells infected with the B95-8 EBV strain. (**E**) The length of the reads obtained after sequencing of the library generated with M81-infected B cells is plotted against the number of these reads. (**F**) Same as in (**E**) but with cells infected with the B95-8 EBV strain. (**G**) The graph shows the distribution of ribosome-protected fragments around the start and stop codons of strongly expressed cellular genes after a 5 min incubation with harringtonine (top) or treatment with cycloheximide (bottom) of a M81-infected sample. (**H**) Same as in (**G**) but with libraries prepared from B95-8-infected LCLs. CHX: cycloheximide, Harr: harringtonine

Supplementary Figure 3

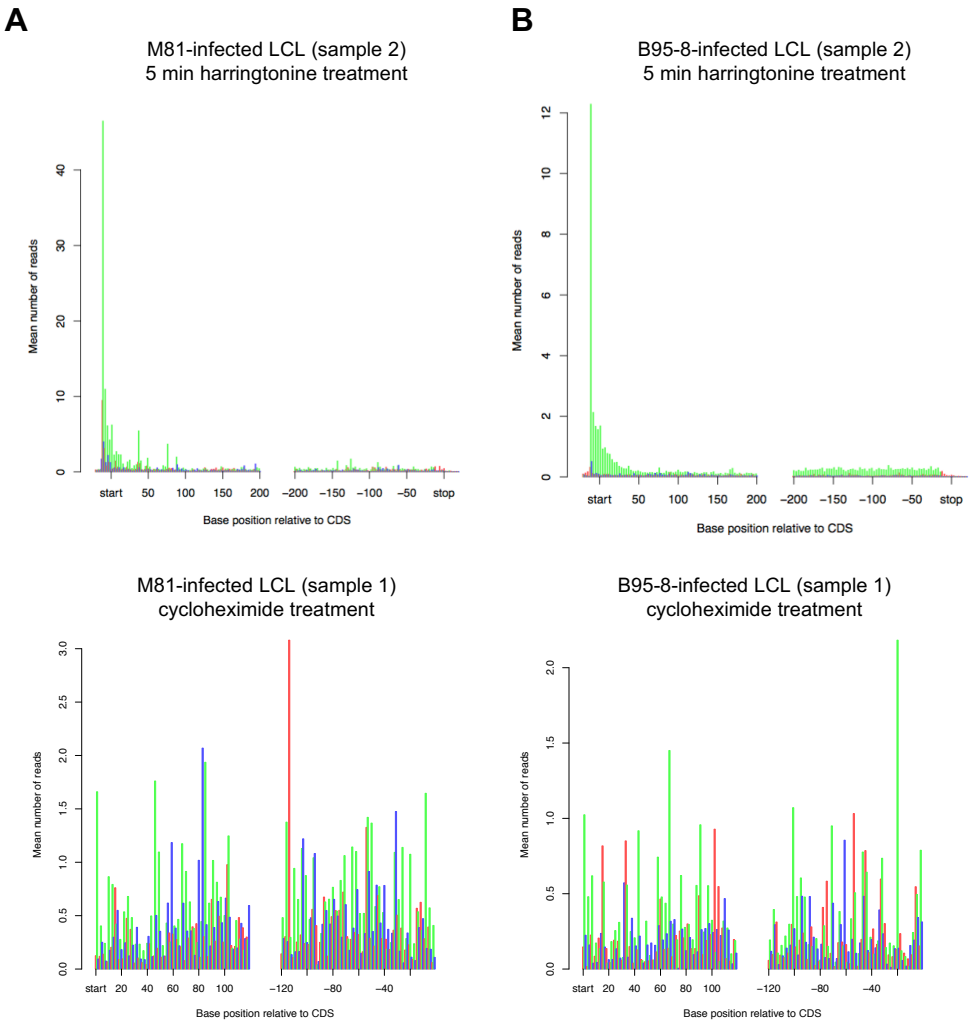

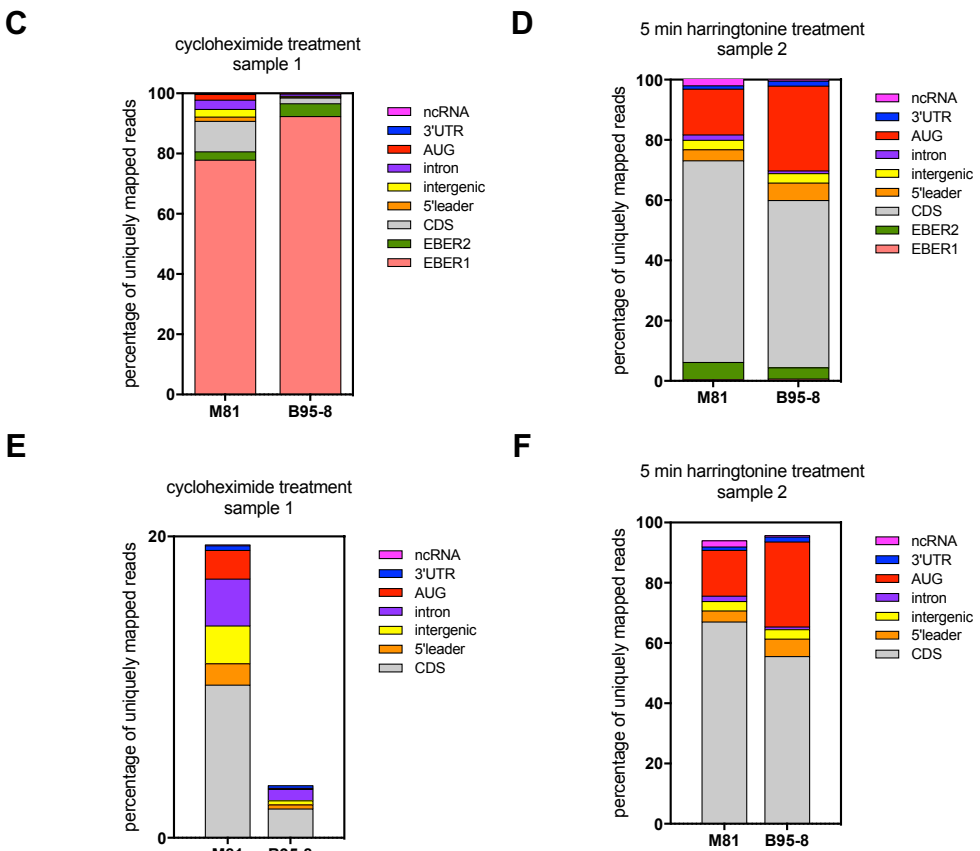

Supplementary Figure 3: Triplet periodicity and read distribution within the gene loci. (**A**) The analysis was performed with LCLs infected with M81 and treated with harringtonine for 5 min (top) or treated with cycloheximide (bottom). The plot shows the average number of reads centered on either of the three reading frames after the start codon and before the stop codon (Red bars: reads centered on frame 0, Green bars: on frame 1, Blue bars: on frame 2). (**B**) Same as in (**A**) but with libraries prepared from LCLs infected with B95-8. (**C**) The figure shows the mapping of sequences from cycloheximide-treated LCLs generated with M81 or B95-8 to the viral genome, according to their distribution within a viral gene locus. A large number of reads mapped to the EBER1 and EBER2 genes. The EBER RNAs form a complex with multiple proteins that presumably protected them from nuclease digestion. The remaining sequences mapped to the different parts of the viral gene loci. These include 5'leader, AUG initiation site and open reading frame (here referred to as coding DNA sequence (CDS)), introns, 3' untranslated regions (3'UTR), as well as DNA located between viral genes (intergenic) and genes that encode ncRNA. When reads simultaneously mapped to multiple elements, the given preference order was AUG, CDS, 5'leader, 3'UTR, ncRNA, intron, intergenic. (**D**) The figure shows the results of the analysis described in (**C**) but after treatment with harringtonine. (**E**) Same as in (**C**) but with the mapping to the EBER region removed. (**F**) Same as in (**D**) but with the mapping to the EBER region removed.

Supplementary Figure 4

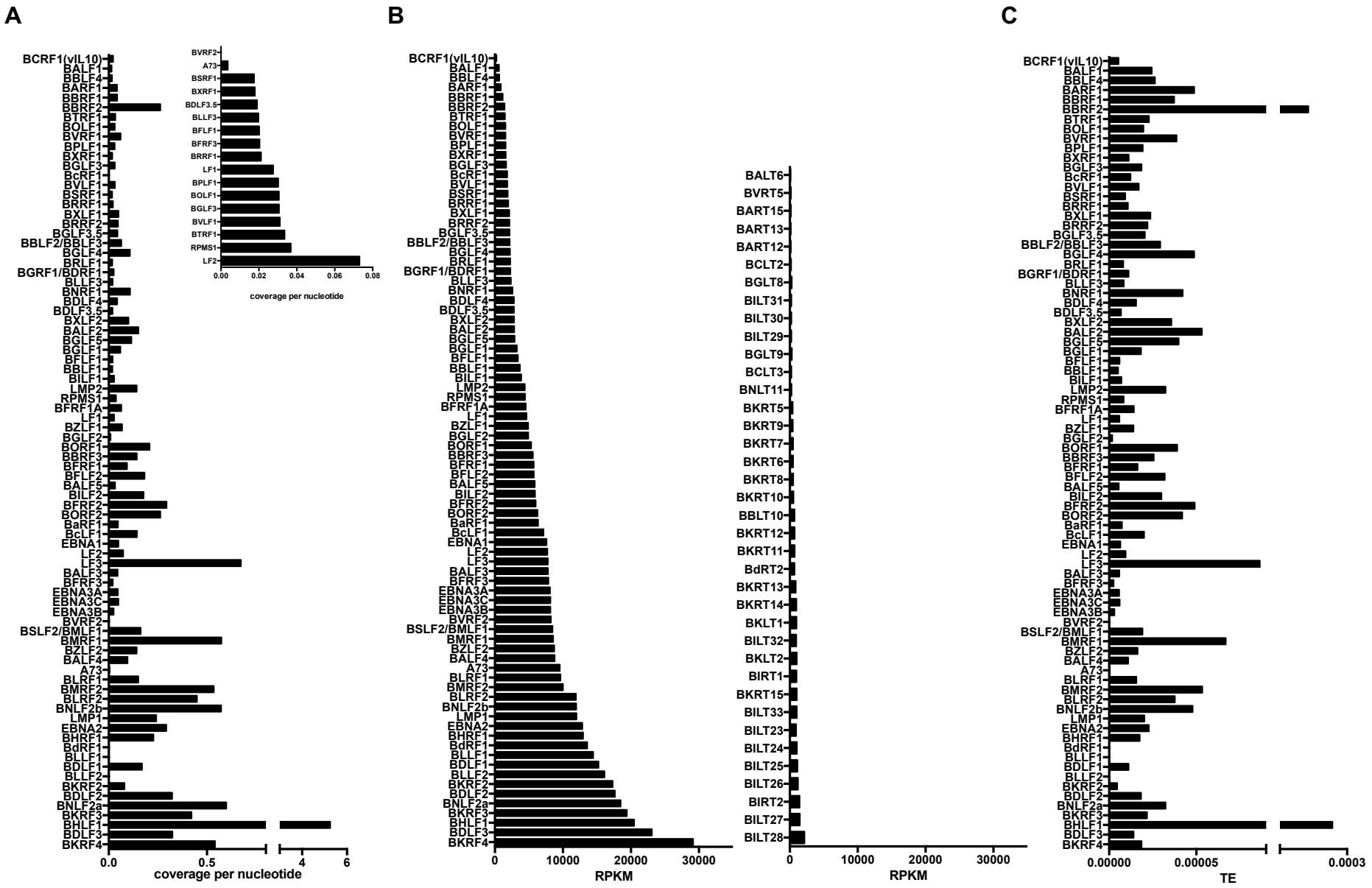

Supplementary Figure 4: Viral transcripts are translated with different efficiencies in M81-infected LCLs. (**A**) The graph of bars shows the per nucleotide normalized read coverage in the ribosome profiling library generated with cycloheximide-treated LCLs. The inset shows the results for viral genes with very low coverage. (**B**) The vertical graph of bars shows the expression level of viral genes in cells derived from sample 1 and infected with M81 EBV, ranked by decreasing abundance. The expression level is plotted as reads per kilobase per million mapped reads (RPKM). The RPKM values for the newly identified antisense lytic transcripts are shown on the right. We show only the genes with a number of reads superior to 500 RPKM (**C**) The graph of bars shows the translation efficiency (TE) of viral genes in cells infected with M81. TE is displayed as the ratio between the ribosome protected fragments in the coding region of a gene and the transcription level of these genes in RPKM. This transcriptome and the cycloheximide ribosome profiling library were generated from the same EBV-infected cells.

Supplementary Figure 5

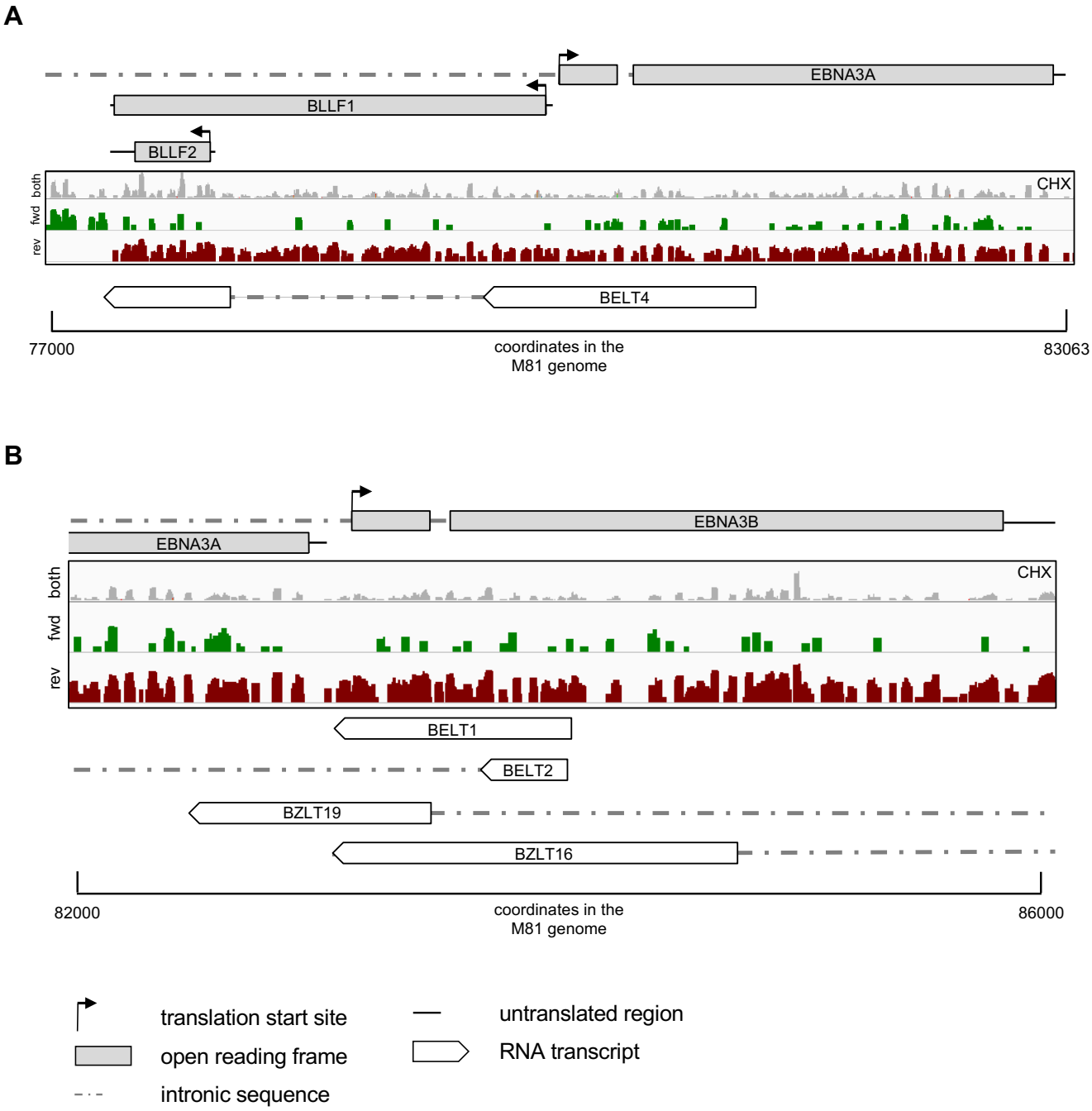

Supplementary Figure 5: Association of transcripts antisense to EBNA3A and EBNA3B with ribosomes. (**A**) The grey reads show the total ribosome protected fragments (RPFs) from an M81-infected sample treated with cycloheximide that mapped to the viral segment that contains the EBNA3A gene. The rightward reads are shown in green, the leftward reads in red. The panel also shows a schematic map of EBNA3A, some of the newly identified antisense transcripts and their coordinates in the genome (**B**) Same as in (**A**) but for the EBNA3B gene.

Supplementary Figure 6

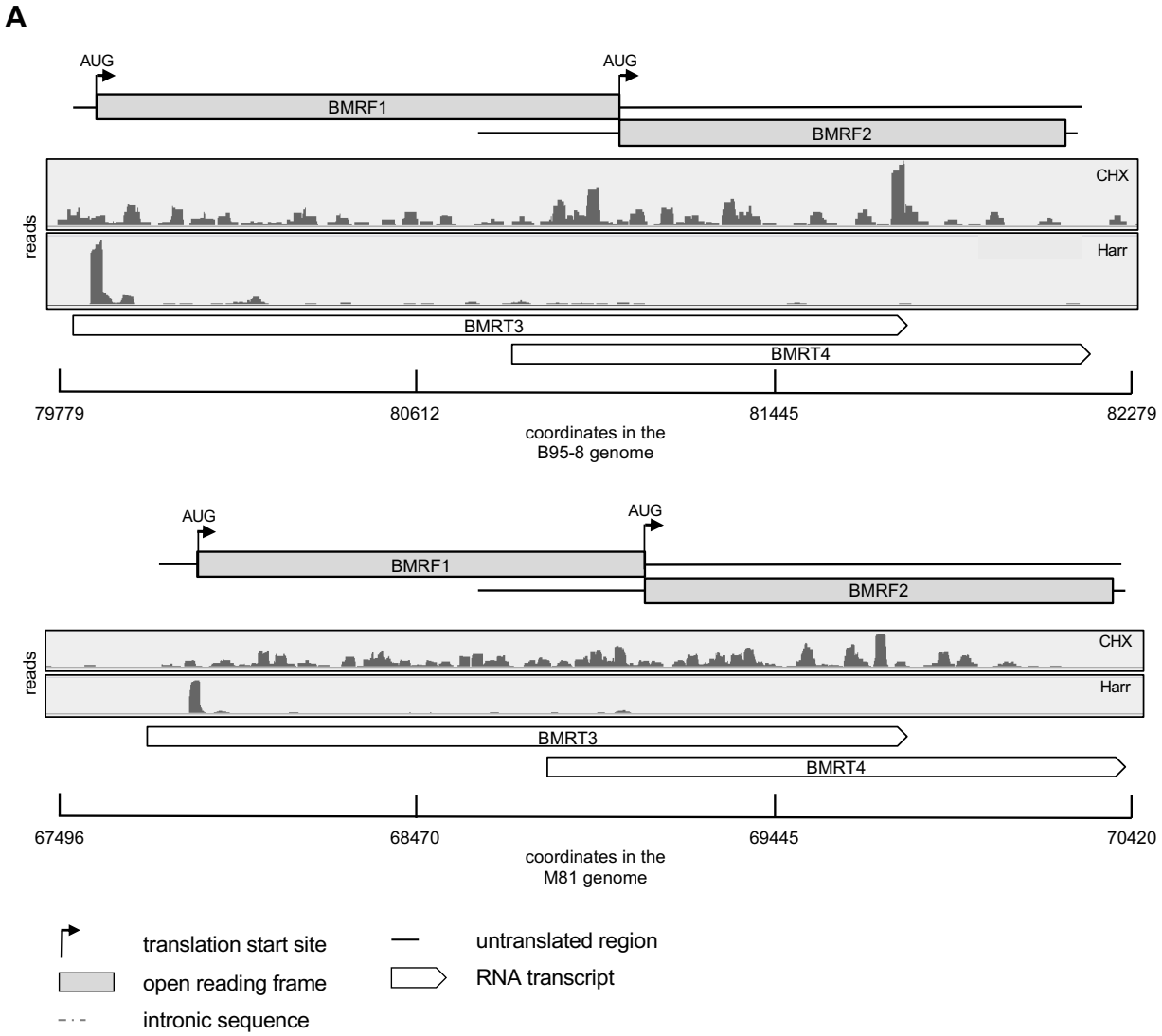

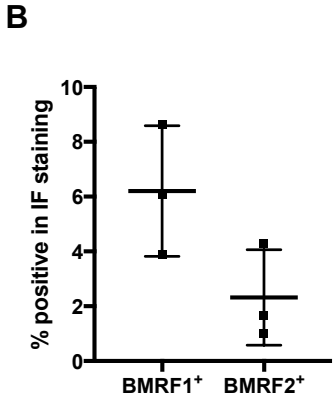

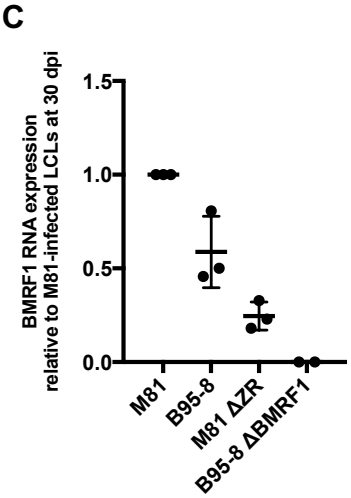

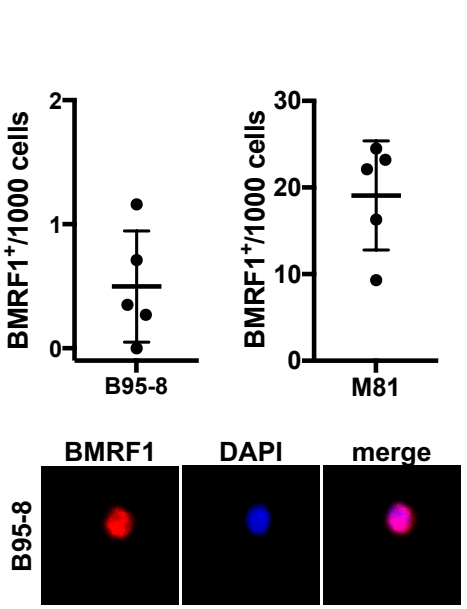

Supplementary Figure 6: Ribosome distribution in the BMRF1 and BMRF2 transcripts in LCLs. (**A**) Details of the ribosome profile around the BMRF1 coding region in B cells infected either with B95-8 (*top*) or M81 (*bottom*) and treated with cycloheximide (CHX) or harringtonine (Harr). The panel also shows the two novel transcripts identified by O'Grady et al. (1) (**B**) The dot plot shows the percentage of BMRF1 and BMRF2 positive cells in M81-transformed LCLs. (**C**) This dot plot shows the abundance of BMRF1 transcripts in LCLs generated with different viral strains as determined by RT-qPCR. M81 is a lytic strain, whereas B95-8 is predominantly latent. M81 ΔZR is a M81 mutant incapable of lytic reactivation. B95-8 ΔBMRF1 is a B95-8 mutant that carries a deletion of the BMRF1 gene. The results are given relative to the BMRF1 RNA expression levels recorded in M81-infected cells at day 30 post-infection (dpi). (**D**) We performed immunostains with antibodies specific for BMRF1. The percentage of positive cells within the LCLs was quantified in both strains and is given in the dot plots. An example of a BMRF1-positive cell infected with B95-8 is shown below. The B95-8-transformed LCLs were all BMRF2 negative.

Supplementary Figure 7

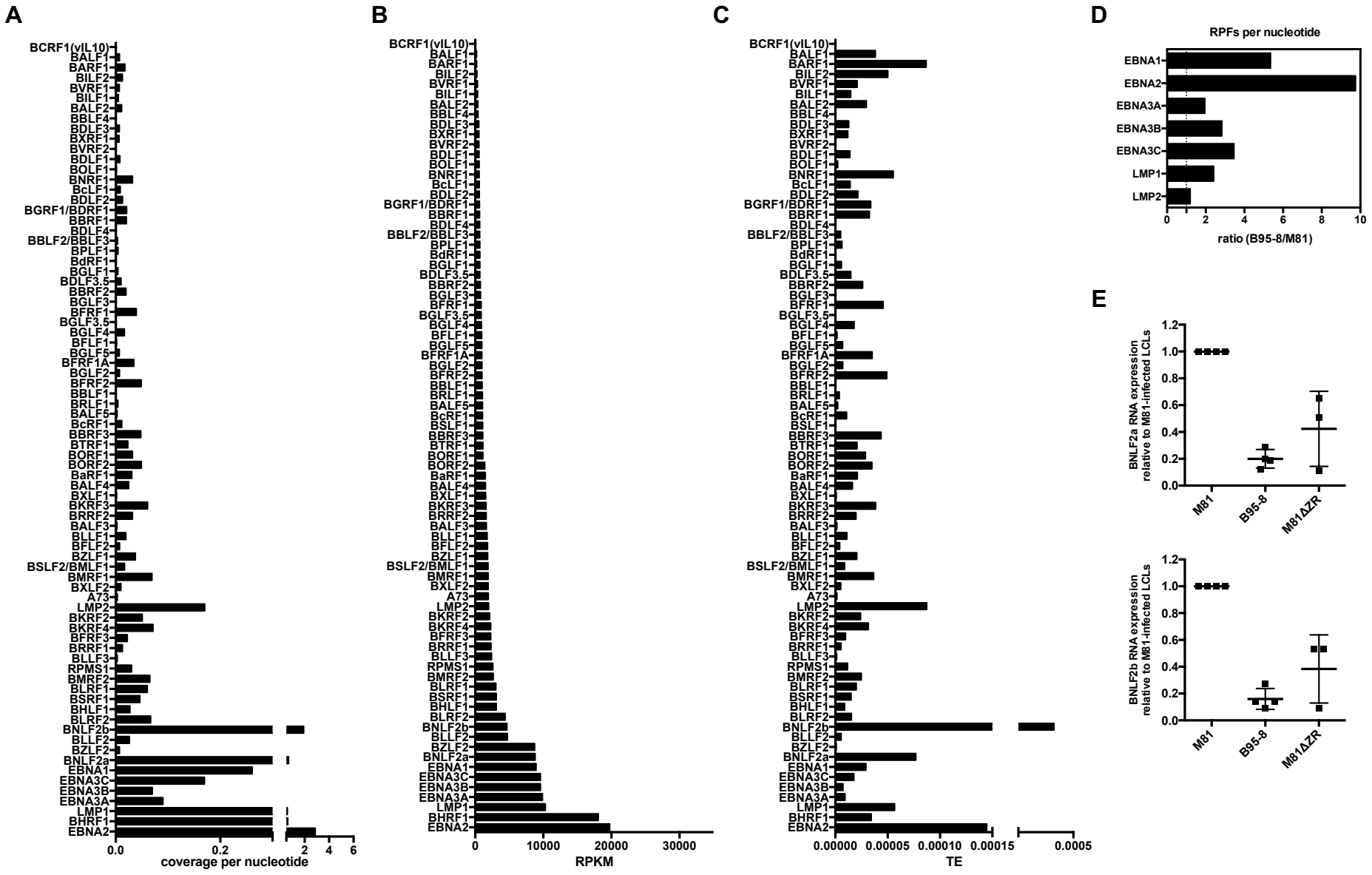

Supplementary Figure 7: Viral transcripts are translated with different efficiencies in B95-8-infected LCLs. (**A**) The graph of bars shows the per nucleotide normalized read coverage derived from the cycloheximide-treated ribosome profiling library. (**B**) The vertical graph of bars shows the expression level of viral genes in cells derived from sample 1 and infected with B95-8 EBV, ranked by decreasing abundance. The expression level is plotted as reads per kilobase per million mapped reads (RPKM). (**C**) The graph of bars shows the translation efficiency (TE) of viral genes in cells infected with B95-8. The TE is displayed as the ratio between the ribosome protected fragments in the coding region of a gene and the transcription level of these genes in RPKM. This transcriptome and the cycloheximide ribosome profiling library were generated from the same EBV-infected cells. (**D**) The graph of bars shows a comparative analysis of latent gene translation as the ratio of RPF coverage per nucleotide in cells infected with either M81 or B95-8. (**E**) qPCR analysis showing expression of BNLF2a and BNLF2b in cells infected with M81, M81/ΔZR or B95-8. The results are given relative to M81.

Supplementary Figure 8

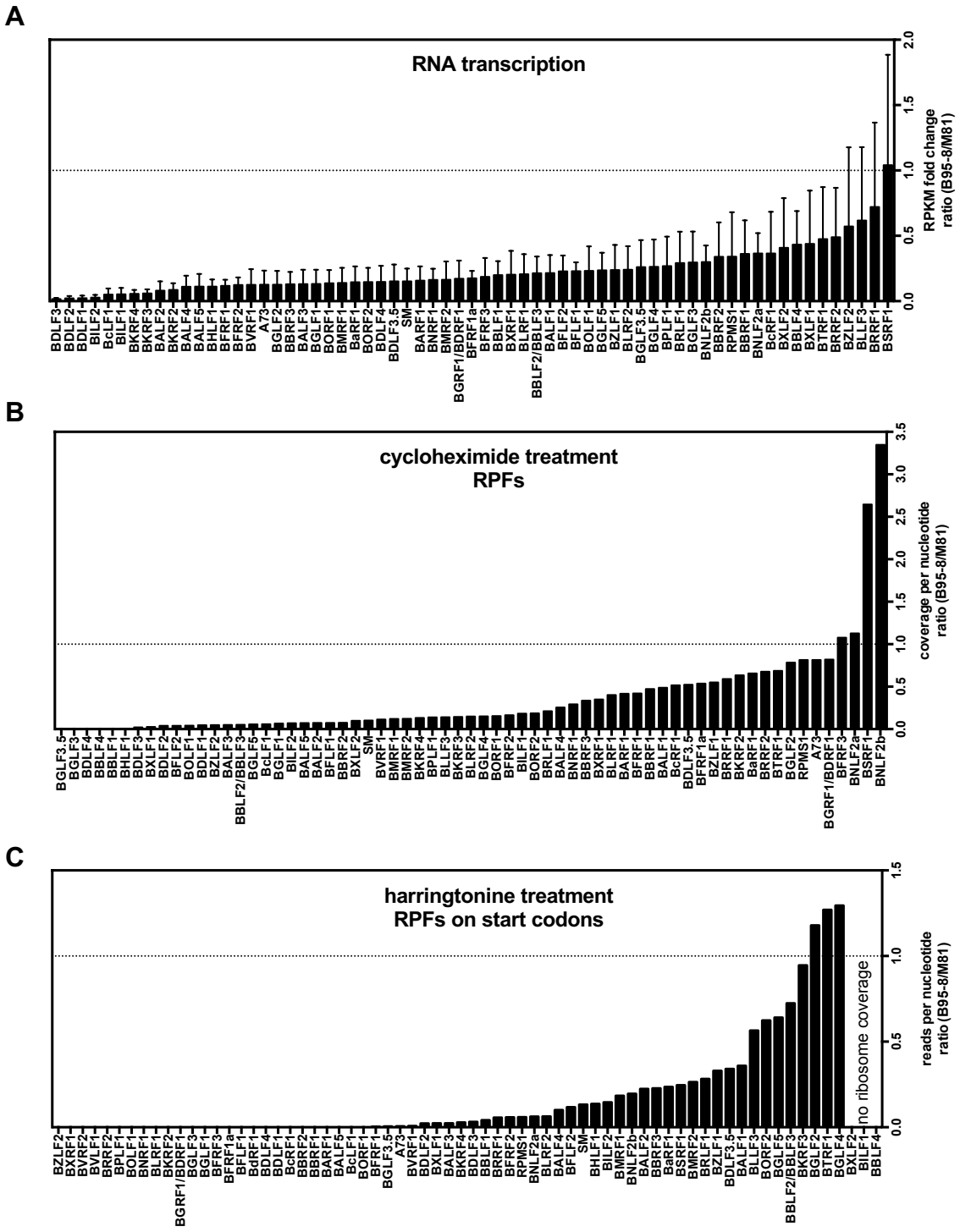

Supplementary Figure 8: Lytic gene transcription and translation in cells infected with the mainly latent B95-8 EBV strain. (**A**) The graph of bars shows a comparative analysis of lytic gene transcription in cells infected with either M81 or B95-8. Two independent libraries were sequenced. The bars give the mean relative fold change between cells infected with B95-9 or with M81 and the standard deviation of gene expression levels. (**B**) The graph of bars shows a comparative analysis of lytic gene translation in cells infected with either M81 or B95-8 and treated with cycloheximide. The bars indicate the ratios of ribosome-protected fragments obtained from cells infected with either type of virus, both expressed as coverage per nucleotide. Only reads mapping to the open reading frames of the respective genes were considered. (**C**) Same as in (**B**) but with cells treated with harringtonine. The analysis was restricted to reads that mapped to the start codon of the viral genes.

Supplementary Figure 9

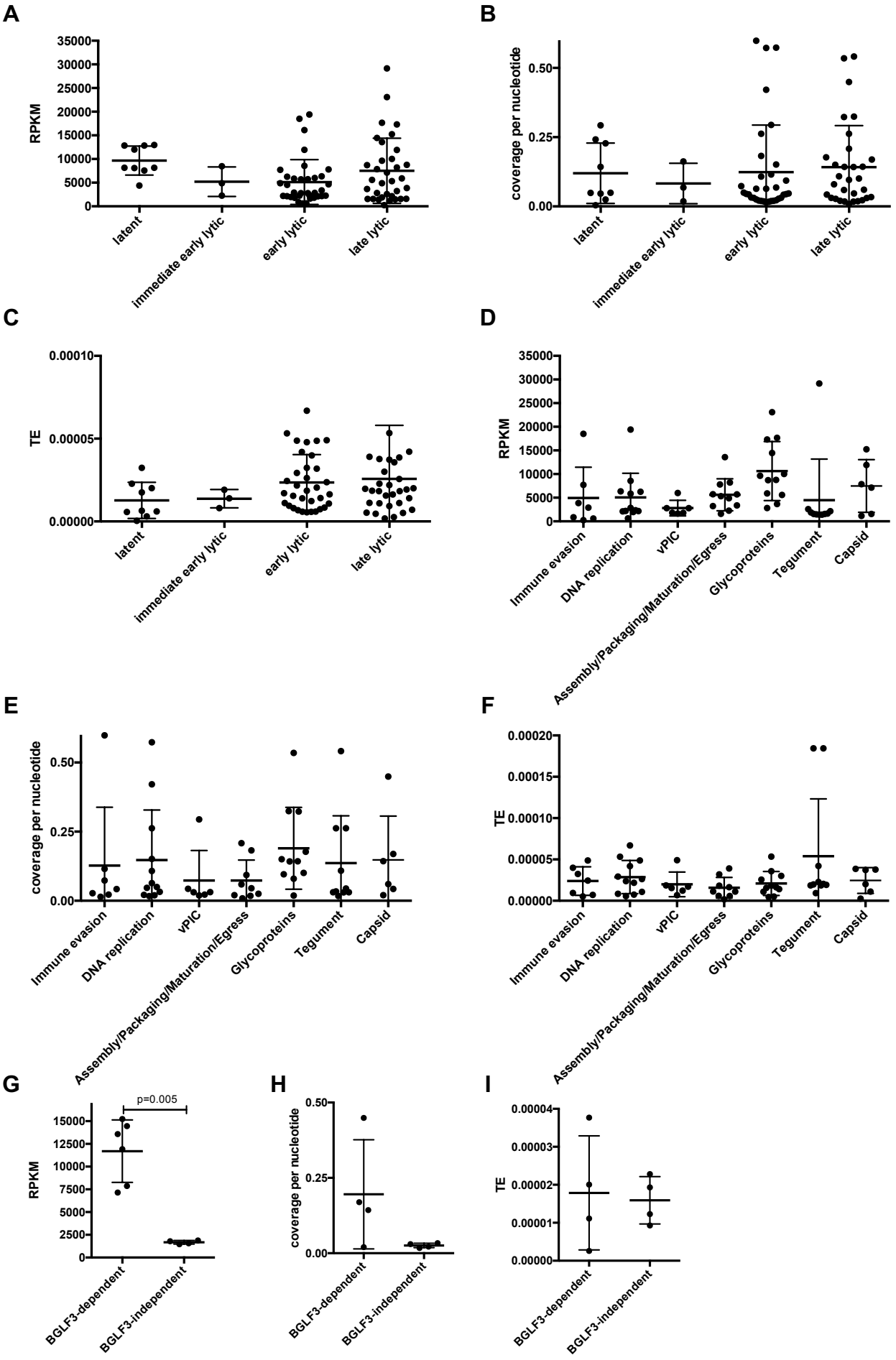

Supplementary Figure 9: Transcription and translation of different classes of viral transcripts in M81-infected B cells. (**A**) The dot plots show the transcription, ribosome coverage and translation efficiency levels of viral genes in the LCL generated with B cells of sample 1 after infection with M81, grouped according to their kinetic of expression (**A, B, C**) or viral function (**D, E, F**). Transcription levels are given as RPKM values, the ribosome coverage values are shown normalized to ORF length. The translation efficiency (TE) is displayed as the ratio between the ribosome protected fragments in the coding region of a gene and the transcription level of these genes in RPKM. We have also included in this analysis the components of the recently described viral pre-initiation complex (vPIC) (2). In (**G**), (**H**), and (**I**), the analysis is restricted to lytic genes whose expression is dependent on BGLF4 and distinguishes between transcripts that are dependent or independent of BGLF3, as described by McKenzie et al. (3).

Supplementary Figure 10

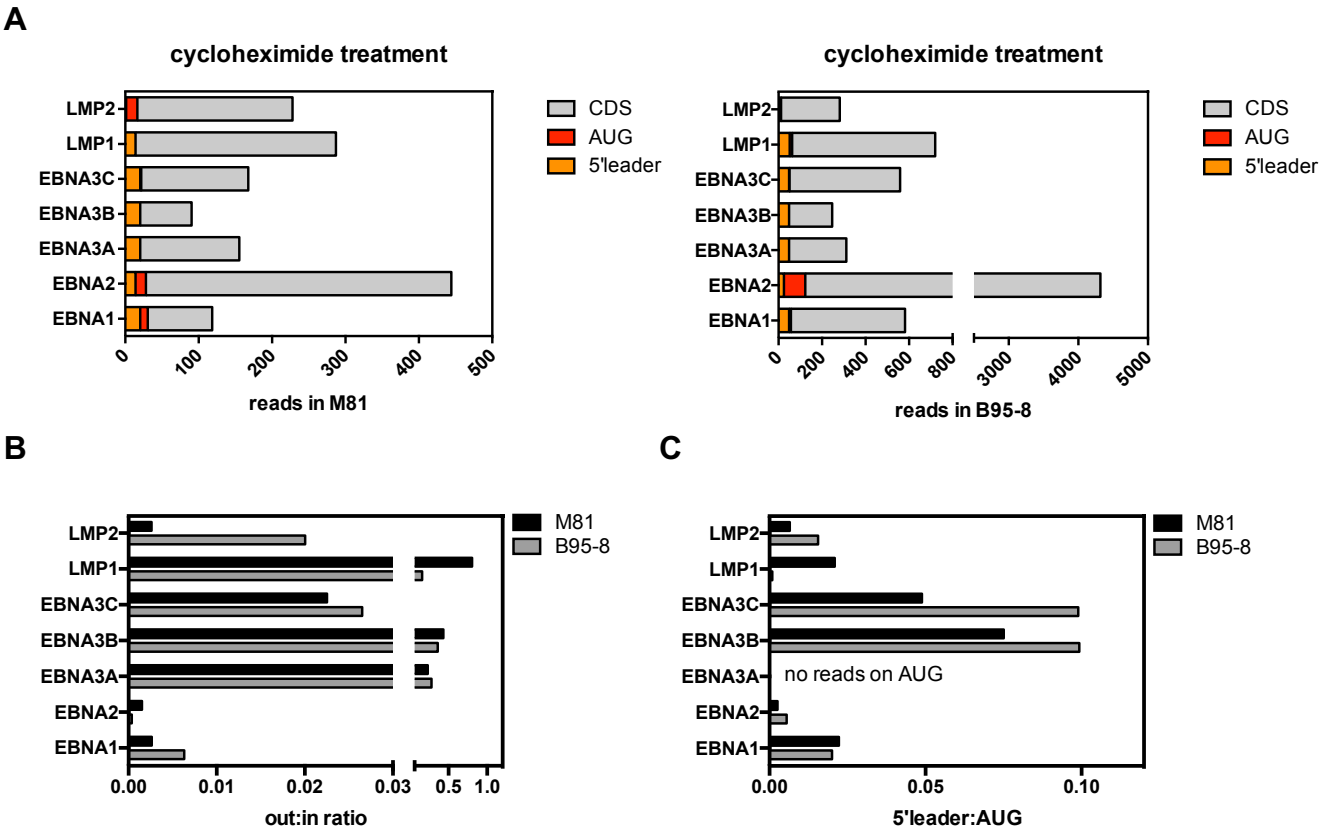

Supplementary Figure 10: Ribosome footprints on latent EBV transcripts in LCLs infected with B95-8 and M81. (**A**) Read distribution on latent genes in libraries generated with the cycloheximide-treated LCLs. The reads are classified according to their localization within the mRNA transcripts: coding DNA sequence (CDS), annotated start codon (AUG), 5' leader of the mRNA transcript (5'leader). LMP2A and LMP2B are pooled together and given as LMP2. EBNA-LP was omitted due to the repetitive nature of its exons that precludes accurate mapping. The reads that map to the U exon are shared by the members of the EBNA3 family genes and by EBNA1 and cannot be distinguished. Therefore, we ascribed one fourth of the total reads to each gene. Similarly, we divided the reads that mapped to the Y2 exon between the latent genes that carry it. (**B**) Ratios of reads mapping to the 5'leader vs the AUG and the open reading frame (combined) of the latent genes (out:in ratio). (**C**) Ribosomes are captured in the 5'leader. Ratios of reads covering the 5'leader of the latent genes to the reads covering their start codons. EBNA3A did not have any AUG coverage in any of the three libraries generated for LCLs treated with harringtonine. Thus, the 5'leader:AUG ratio is meaningless. EBNA1, 3B and 3C show a large excess of reads that map to their 5'leader.

Supplementary Figure 11

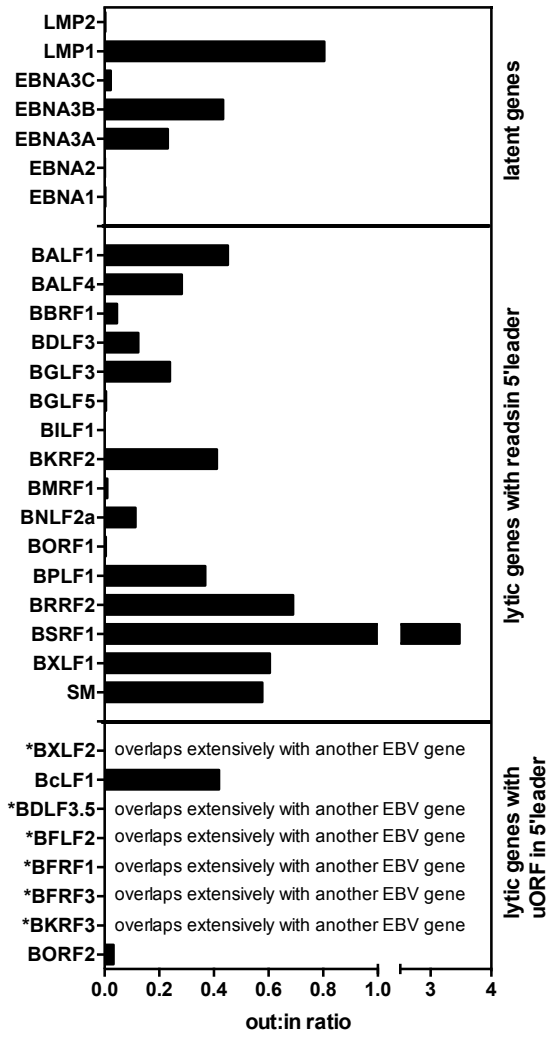

Supplementary Figure 11: Influence of the 5'leader on the translation of lytic genes. Ratios of reads mapping to the 5'leader of the respective genes to reads mapping to the start codon and within the open reading frame (plotted as out:in ratios) in the library generated with LCLs transformed with M81 and treated with cycloheximide. The gene list is sorted according to the presence or absence of ribosome footprints in the 5'leaders and the presence of uORFs. *The 5'leader of these genes overlaps with the CDS of other genes and as a consequence mapping of the reads in cells treated with cycloheximide can be ambiguous. Therefore, no ratio calculations could be performed for these genes.

Supplementary Figure 12

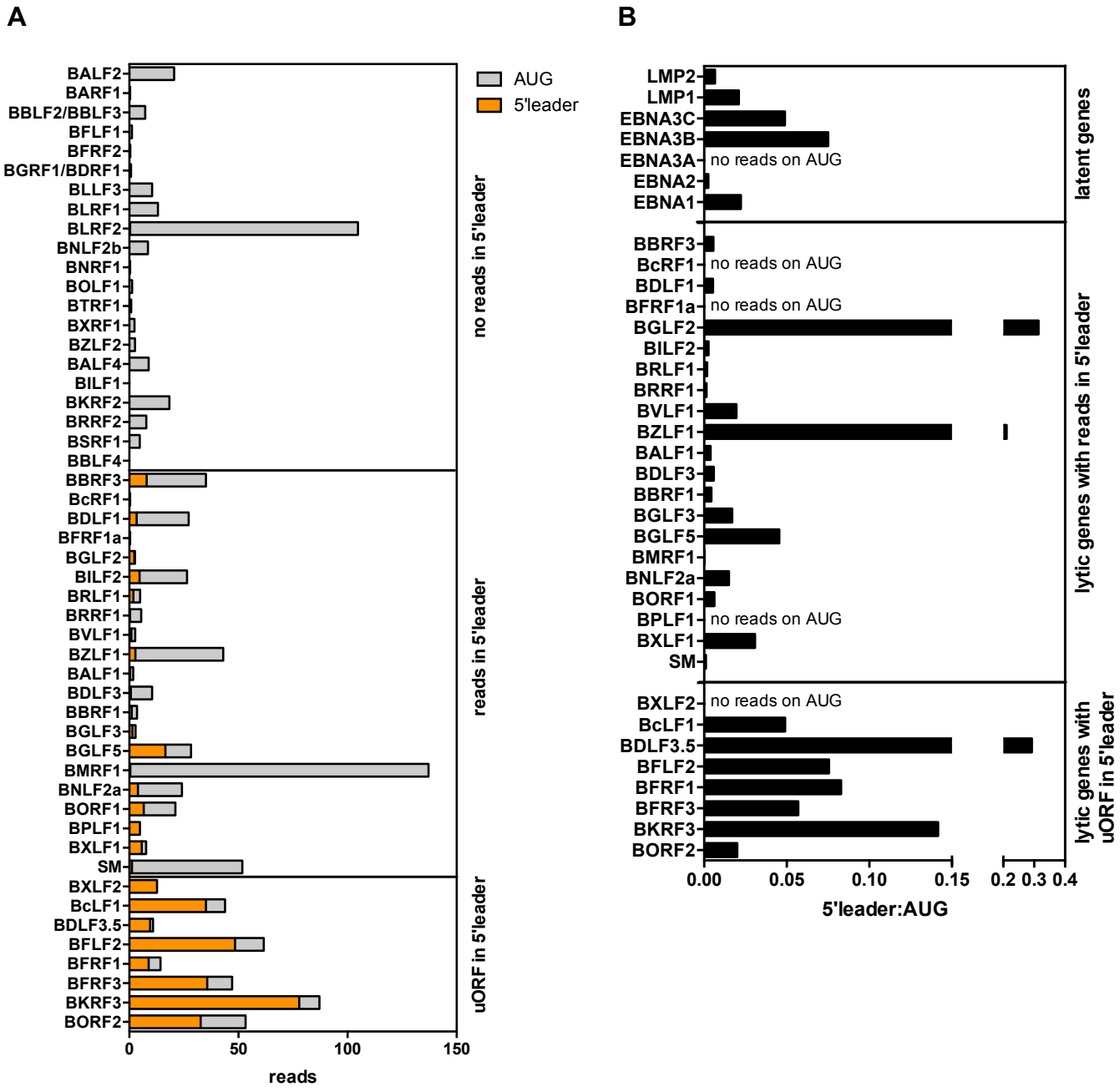

Supplementary Figure 12: Efficacy of ribosome trapping in the 5'leader of lytic transcripts. (**A**) The figure shows the distribution of ribosome footprints within lytic genes in M81-transformed LCLs treated with harringtonine. The lytic genes are classified according to the presence or absence of ribosome footprints in the respective 5'leader and the existence of 5'leader-regulatory elements. (**B**) Ratios of reads mapping to the 5'leader to reads mapping to the annotated start codons of the respective genes. The data presented are based on the analysis of three harringtonine-treated libraries. AUG: annotated start codon.

Supplementary Figure 13

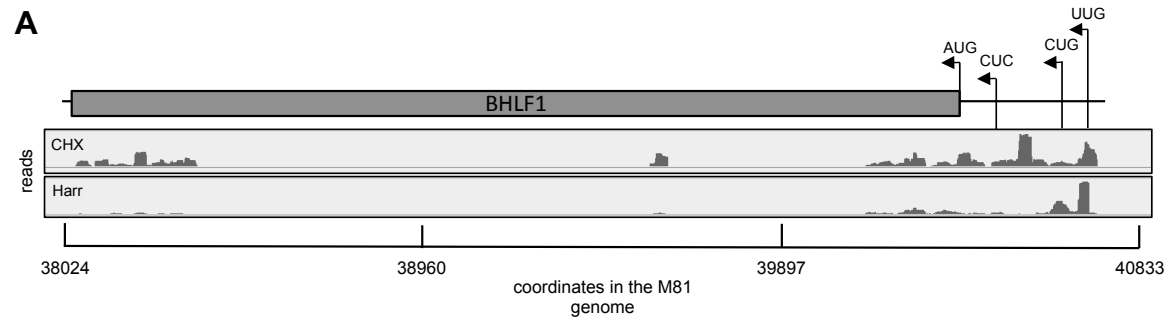

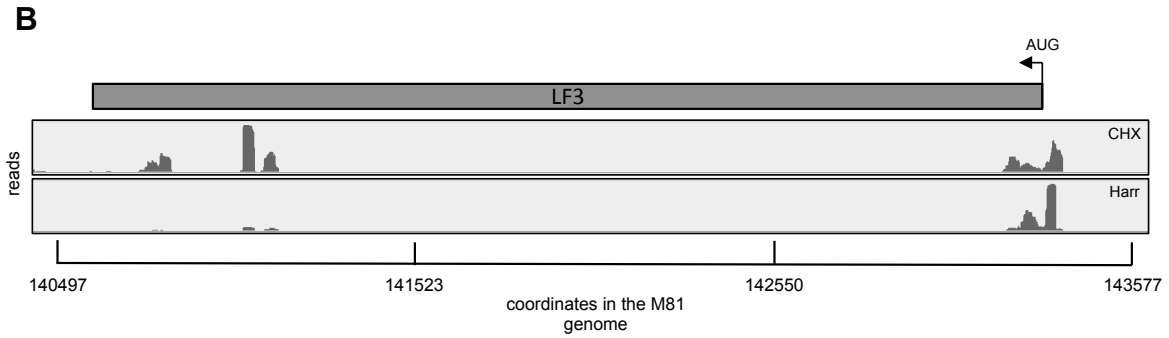

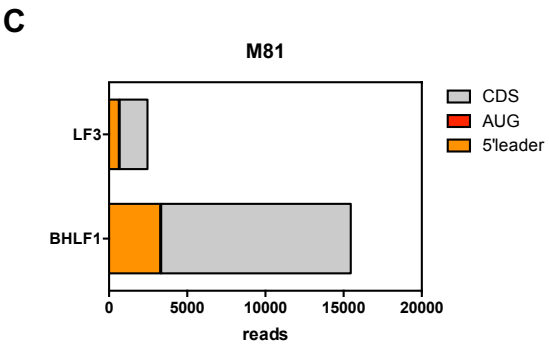

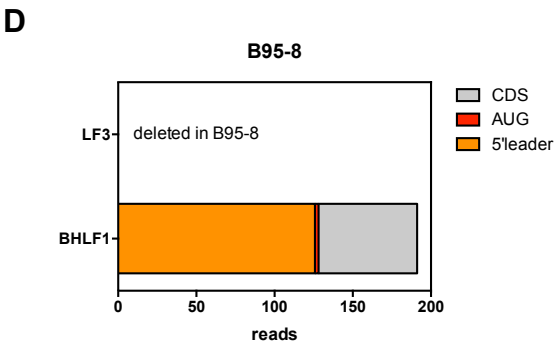

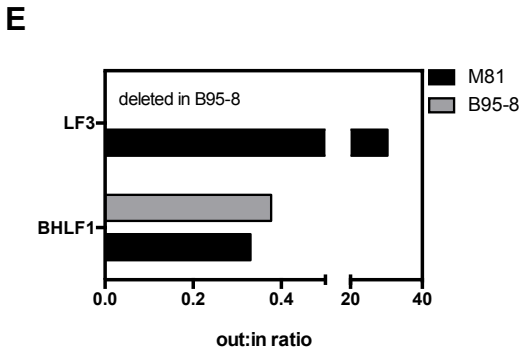

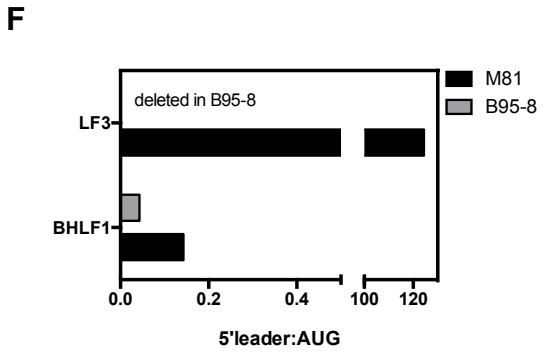

Supplementary Figure 13: Ribosome footprints on the BHLF1 and LF3 transcripts. (**A**) The figure shows the reads mapping around the BHLF1 gene in M81 LCLs treated with cycloheximide (CHX) or harringtonine (Harr). Many reads mapped to three uORFs, all non-canonical, 5' of the translation initiation site. (**B**) The figure shows the ribosome profile of the LF3 transcript in LCLs infected with M81. (**C**) Read distribution on BHLF1 and LF3 in the library generated from cycloheximide-treated M81-infected LCLs. (**D**) Read distribution on BHLF1 in the library generated from cycloheximide-treated B95-8-infected LCLs. The LF3 gene is deleted in B95-8. (**E**) Ratios between reads mapping within the 5'leader (out) to the start codon and coding region (in) of the respective gene. (**F**) Ratios of reads mapping to the 5'leader to reads mapping to the annotated start codons of the BHLF1 and LF3 genes in harringtonine-treated libraries in the respective EBV strains.

Supplementary Figure 14

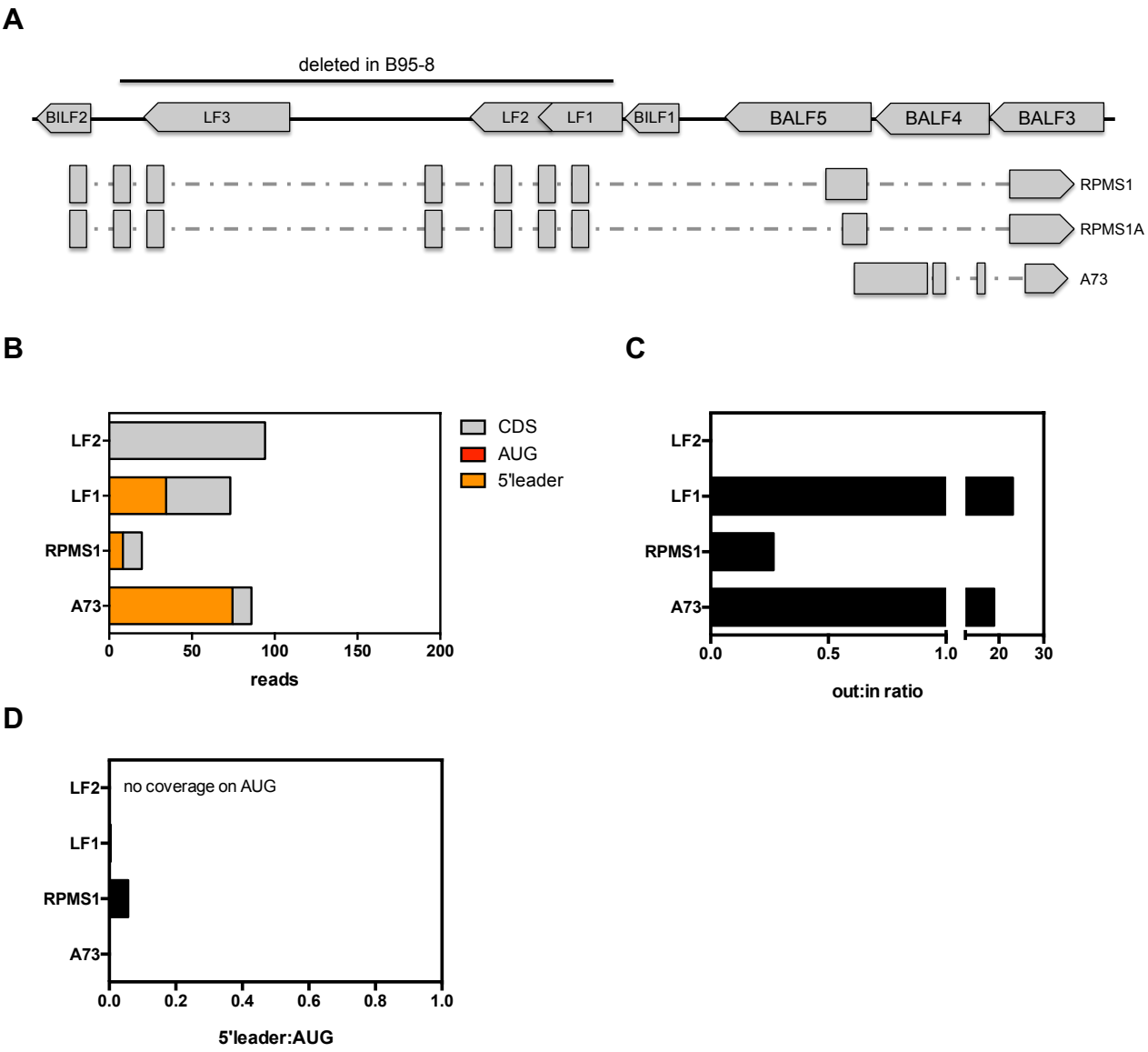

Supplementary Figure 14: Ribosome profiling of the BART transcripts. (**A**) This schematic overview describes the EBV BART region with its encoded genes. The rightward transcripts for RPMS1, RPMS1A and A73 are also depicted. The drawing is not to scale. (**B**) Total read distribution on the BART genes in the library generated with M81-infected LCLs treated with cycloheximide. (**C**) Reads mapping within the 5'leader (out) and start codon and the coding region (in) of the respective gene are plotted as out:in ratios. We used the sequences generated from cycloheximide-treated LCLs. (**D**) Ratios of reads mapping to the 5'leader to reads mapping to the annotated start codons (AUG) of the respective genes in harringtonine-treated libraries in M81 were calculated.

Supplementary Figure 15

A

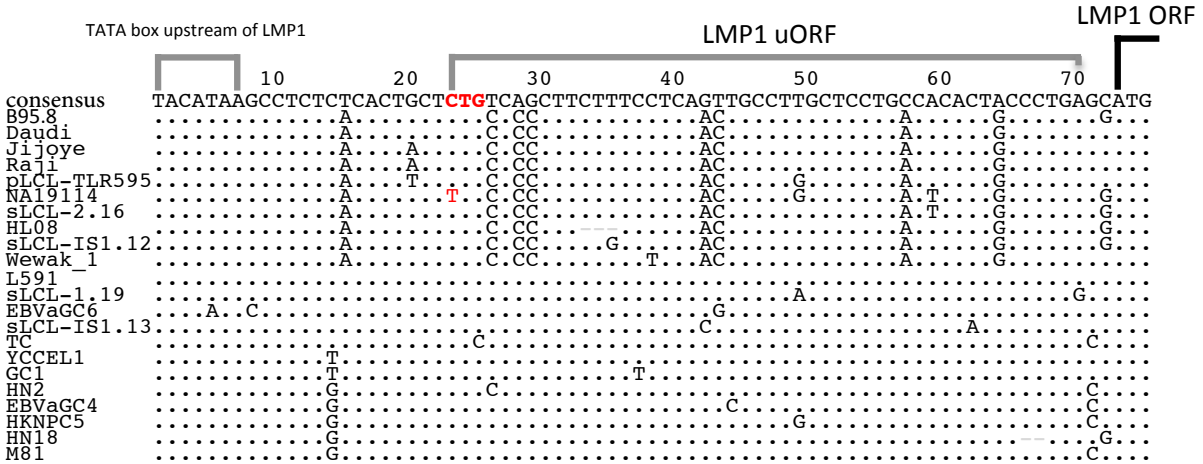

B

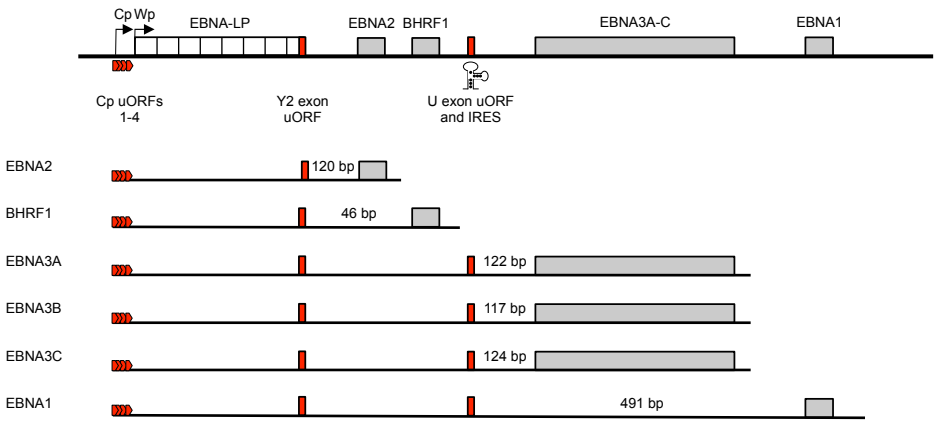

C

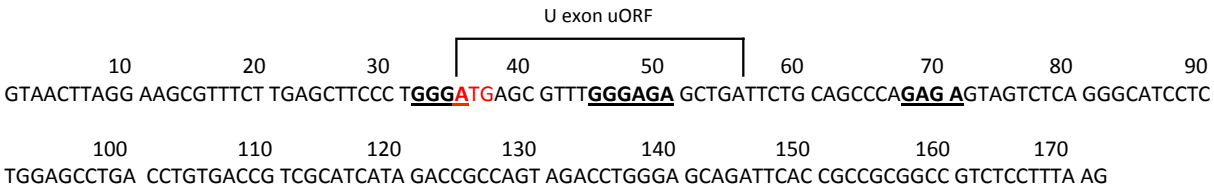

Supplementary Figure 15: EBV's uORFs are well conserved across different EBV strains. (**A**) The alignment shows the sequence variation of the LMP1 uORF. The sequences with polymorphisms in and around the LMP1 uORF are shown. Black dots indicate conserved nucleotides, light grey dashes indicated nucleotide deletions. (**B**) *Top* Overview over the EBV genome encompassing the EBNA transcription unit. Included are the Cp and Wp promoters that drive the transcription of the EBNA genes. The IRES in the U exon is also indicated. *Bottom* The spliced transcripts of the EBNA genes are shown. Upstream open reading frames (uORFs) included in the leader region of the EBNA transcripts are shown in red. The distance between the last uORF and the main ORF is indicated but the drawings are not to scale. bp: basepair (**C**) The figure shows the nucleotide sequence of EBV's U exon. The IRES consensus sequences identified by Isaksson et al. (4) are indicated in bold letters. The start codon of the U exon uORF is highlighted in red

References

1. O'Grady, T., Wang, X., Honer Zu Bentrup, K., Baddoo, M., Concha, M. and Flemington, E.K. (2016) Global transcript structure resolution of high gene density genomes through multi-platform data integration. *Nucleic acids research*.
2. Aubry, V., Mure, F., Mariame, B., Deschamps, T., Wyrwicz, L.S., Manet, E. and Gruffat, H. (2014) Epstein-Barr virus late gene transcription depends on the assembly of a virus-specific preinitiation complex. *Journal of virology*, **88**, 12825-12838.
3. McKenzie, J., Lopez-Giraldez, F., Delecluse, H.J., Walsh, A. and El-Guindy, A. (2016) The Epstein-Barr Virus Immunoevasins BCRF1 and BPLF1 Are Expressed by a Mechanism Independent of the Canonical Late Pre-initiation Complex. *PLoS pathogens*, **12**, e1006008.
4. Isaksson, A., Berggren, M. and Ricksten, A. (2003) Epstein-Barr virus U leader exon contains an internal ribosome entry site. *Oncogene*, **22**, 572-581.

Supplementary Table 1: Characteristics of the sequenced RNA libraries

The first column identifies the blood sample used for the generation of the sequenced cell lines, the second column indicates the type of sequencing experiment performed, column three indicates the virus type used for the generation of the B cell lines, column four indicates the type of treatment of the cell lines and column five notes the type of RNA used for the generation of the sequencing libraries and the sixth column shows the total number of reads sequenced in each sample. The seventh column lists all reads remaining following linker removal, the eighth column shows the number of reads remaining in each sample after rRNA sequence removal, the ninth column lists the number of reads that aligned to the human and viral genomes, the tenth column lists the reads that mapped to the viral genome and the last column indicates the number of these reads that were mapped to the EBER genes. RPF: ribosome protected fragments

blood sample	experiment type	Virus used	pretreatment	RNA type	sequenced reads	reads following clipping	reads following rRNA removal	mapped reads	total viral reads	EBER reads
sample 1	total RNA sequencing	B95-8	no pretreatment	total RNA	306,089,144	not done	not done	285,179,549	823,601	not done
sample 1	ribosome profiling	B95-8	cycloheximide	RPF	49,874,563	44,682,658	29,039,482	15,514,135	475,700	458,764
sample 1	ribosome profiling	B95-8	2 min harringtonine	RPF	17,476,623	11,038,224	4,170,313	2,439,254	21,287	19,593
sample 1	total RNA sequencing	M81	no pretreatment	total RNA	269,552,432	not done	not done	256,945,000	1,117,298	not done
sample 1	ribosome profiling	M81	cycloheximide	RPF	33,592,695	30,042,652	16,881,387	9,945,378	393,252	313,907
sample 1	ribosome profiling	M81	2 min harringtonine	RPF	27,108,396	24,591,719	11,160,336	5,224,299	18,100	3,916
sample 2	total RNA sequencing	B95-8	no pretreatment	total RNA	188,850,498	not done	not done	180,355,254	959,400	not done
sample 2	ribosome profiling	B95-8	2 min harringtonine	RPF	45,666,734	39,400,972	15,383,128	8,235,491	15,050	7,930
sample 2	ribosome profiling	B95-8	5 min harringtonine	RPF	49,161,723	45,998,693	7,392,648	3,861,791	5,298	212
sample 2	total RNA sequencing	M81	no pretreatment	total RNA	170,847,650	not done	not done	162,704,318	969,688	not done
sample 2	ribosome profiling	M81	2 min harringtonine	RPF	58,997,731	56,141,014	8,481,210	5,810,660	8,550	1,340
sample 2	ribosome profiling	M81	5 min harringtonine	RPF	35,032,225	33,753,242	6,445,370	3,406,665	3,992	244
producer cell line	ribosome profiling	293-2089	5 min harringtonine	RPF	18,763,156	12,997,976	6,231,563	3,246,322	258,258	19,945

Supplementary Table 2: Classification of the Kozak sequences surrounding EBV's upstream open reading frames

Kozak sequence signal strength classification

++	[**A/G**]CCaug**G**
+	[**A/G**]NNaug**G**[notU]
-	all other sequences

uORF	uORF length [aa]	Sequence around the uORF start codon	classification
Cp uORF1‡	1	**A**AAaug**U**A	-
Cp uORF2	2	**C**AGaug**G**C	-
Cp uORF3	1	**G**CCaug**U**A	-
Cp uORF4	1	**A**UCaug**U**A	-
BHLF1 uORF1	36	**C**CCcuc**C**C	-
BHLF1 uORF2	20	**G**GCcug**G**G	-
BHLF1 uORF3	7	**U**CCuug**C**G	-
Y2uORF	7	**A**GGaug**A**A	+
BHRF1 uORF1	14	**G**GCcug**A**A	-
BHRF1 uORF2	74	**C**ATcug**G**A	-
BFLF2 uORF1	30	**U**GGaug**U**C	-
BFLF2 uORF2	12	**G**ACcug**G**U	-
BFRF1 uORF	10	**U**CAuug**C**U	-
BFRF3 uORF1	25	**G**CAacg**C**C	-
BFRF3 uORF2	41	**G**AAuug**C**C	-
UuORF	6	**G**GGaug**A**G	+
BORF2 uORF	17	**G**UGgug**G**A	-
BKRF3 uORF1	45	**A**UCcug**A**A	-
BKRF3 uORF2	27	**A**CCcug**G**A	-
BDLF3.5 uORF	8	**G**AGaug**A**A	+
BcLF1 uORF	11	**G**GCcuc**C**C	-
BXLF2 uORF1	24	**A**GTuug**T**G	-
BXLF2 uORF2	30	**T**GGaug**C**T	-
LMP2A uORF	20	**G**CCuug**U**U	-
LMP1 uORF	15	**G**CUcug**U**C	-

uORF: upstream open reading frame

aa: amino acid

‡: within Cp promoter

Supplementary Table 3: Conservation level of EBV's uORFs

proposed nomenclature	number of strains showing polymorphisms in the uORF start codon/total number of strains analysed	number of strains showing polymorphisms within the uORF/total number of strains analysed
Cp uORF1	0/115	-
Cp uORF2	0/115	-
Cp uORF3	0/115	-
Cp uORF4	0/115	-
BHLF1 uORF1	0/49	26/53
BHLF1 uORF2	0/53	11/53
BHLF1 uORF3	0/53	17/53
Y2uORF	0/120	0/120
BHRF1 uORF1	0/119	11/119
BHRF1 uORF2	1/119	2/119
BFLF2 uORF1	0/124	1/124
BFLF2 uORF2	0/124	1/124
BFRF1 uORF	0/122	0/122
BFRF3 uORF1	1/119	10/119
BFRF3 uORF2	0/119	10/119
UuORF	0/119	0/119
BORF2 uORF	0/119	0/119
BKRF3 uORF1	0/124	7/124
BKRF3 uORF2	1/124	7/124
BDLF3.5 uORF	0/123	1/123
BcLF1 uORF	0/122	2/122
BXLF2 uORF1	0/138	1/138
BXLF2 uORF2	0/138	3/138
LMP2A uORF	0/123	4/123
LMP1 uORF	2/121	22/121

uORF: upstream open reading frame

Supplementary Table 4: Oligonucleotides used in this study.

target gene		primer sequence	probe sequence	strain	assay
BZLF1	fwd	5'-ACGACGTACAAGGAAACC-3'	5'FAM-GCATTCCTCCAGCGATTCTGGCTGTA-3'TAMRA	M81	Taqman*
	rev	5'-CTTGGCCCGGCATTTTCT-3'			
BZLF1	fwd	5'-ACGACGCACACGGAAACC-3'	5'FAM-GCATTCCTCCAGCGATTCTGGCTGTT-3'TAMRA	B95-8	Taqman*
	rev	5'-CTTGGCCCGGCATTTTCT-3'			
EBNA2	fwd	5'-TGCTTAGAAGGTTGTTGGCATG-3'	5'FAM-CCCAACCACAGGTTCAGGCAAAACTTT-3'TAMRA	M81/B95-8	Taqman*
	rev	5'-GCTTAGCCAGTAACCCAGCACT-3'			
EBV polymerase	fwd	5'-CTTTGGCGCGGATCCTC-3'	5'FAM-CATCAAGAAGCTGCTGGCGGCC-3'TAMRA	M81/B95-8	Taqman*
	rev	5'-AGTCCTTCTTGGCTAGTCTGTTGAC-3'			
BMRF1	fwd	5'-CACCATGCTGGTGGTAGATG-3'	-	M81/B95-8	SYBR Green
	rev	5'-GAGATGAGTCTGGGCATGGT-3'			
BNLF2a	fwd	5'-GTGCTTTGCTAGAGCAGCAGT-3'	-	M81/B95-8	SYBR Green
	rev	5'-TTAGTCTGCTGACGTCTGGGT-3'			
BNLF2b	fwd	5'-AGGACTGCATCCAACGCTGC-3'	-	M81	SYBR Green
	rev	5'-CCACACCATCCCAATTCA-3'			
BNLF2b	fwd	5'-AGGACTGCATCCAACGCTT-3'	-	B95-8	SYBR Green
	rev	5'-CCACACCATCCCAATTCA-3'			
BHLF1	fwd	5'-ACCTACATGTCAACCGCCTC-3'	-	M81/B95-8	SYBR Green
	rev	5'-GTGTATTGCTCTCGTTGCCA-3'			
GAPDH	fwd	5'-CAATGACCCCTTCATTGACC-3'	-	M81/B95-8	SYBR Green
	rev	5'-TGGAAGATGGTGATGGGATT-3'			
Firefly luciferase	fwd	5'-GGCTGCAAAAGATCCTCAAC-3'	-	M81/B95-8	SYBR Green
	rev	5'-AATGGGAAGTCACGAAGGTG-3'			
Renilla luciferase	fwd	5'-AACGCGGCCTCTTCTTATTT-3'	-	M81/B95-8	SYBR Green
	rev	5'-ACCAGATTTGCCTGATTTGC-3'			

*Taqman-based RT-qPCR assays were run multiplexed with the commercially available human GAPDH kit from Applied Biosystems. The GAPDH probe was VIC-labeled.

Supplementary Table 5: 5' transcript leader sequences (TLS) synthesized for reporter construct experiments

Column 1 shows the transcript leaders, or their mutated form, that were cloned in front of the Firefly luciferase gene. Column 2 lists the sequences of the uORF-containing 5'leaders indicated in column 1. The uORF sequence is highlighted in red, the mutation introduced to silence the uORF is underlined in the mutant variant. The ATG of the luciferase gene is set in bold type. Each sequence is flanked by enzyme restriction sites (underlined sequences: 5': HindIII and 3': Bsp120I). TLS: transcript leader.

TLS of viral gene	Sequence (5'-3')
LMP1 uORF	AAGCTTGGCAGACCCCGCAAATCCCCCCGGGCCTCCATCCCCAGAAACACGCGTTGCTCTCTCGTAGG CGGCCTACATAAGCCTCTGTCACTGCTCTGTCAGCTTCTTTCCTCAGTTGCCTTGCTCCTGCCACACTA CCCTGACC**ATG**GAAGATGCCAAAAACATTAAGAAGGGCCC
ΔLMP1 uORF	AAGCTTGGCAGACCCCGCAAATCCCCCCGGGCCTCCATCCCCAGAAACACGCGTTGCTCTCTCGTAGG CGGCCTACATAAGCCTCTGTCACTGCTCCGTCAGCTTCTTTCCTCAGTTGCCTTGCTCCTGCCACACTA CCCTGACC**ATG**GAAGATGCCAAAAACATTAAGAAGGGCCC
BFLF2 uORF	AAGCTTATTTAAATCCACACAAGTGGCCAGAGTGGGCAAAACAATCCTCGTGGATGTCACTAAGGAACT GGACGTGGTCCTGCGCATCCACGGCCTTGACCTGGTACAGTCCTATCAAACTTCCCAGGTCTACGTGT GAAAAGTAAAACCG**ATG**GAAGATGCCAAAAACATTAAGAAGGGCCC
ΔBFLF2 uORF	AAGCTTATTTAAATCCACACAAGTGGCCAGAGTGGGCAAAACAATCCTCGTGGACGTCACTAAGGAACT GGACGTGGTCCTGCGCATCCACGGCCTTGACCGGTACAGTCCTATCAAACTTCCCAGGTCTACGTGTG AAAAGTAAAACCG**ATG**GAAGATGCCAAAAACATTAAGAAGGGCCC
BKRF3 uORFs	AAGCTTAGTCTGGCCTCCTTAAATTCACCTAAGAATGGGAGCAACCAGCTGGTCATCAGCCGCTGCGC AAACGGACTCAACGTGGTCTCCTTCTTTATCTCCATCCTGAAGCGAAGCAGCTCCGCCCTCACGAGCC ATCTCCGTGAGTTGTTAACCACCCTGGAGTCTCTTTACGGTTCATTCTCAGTGGAAGACCTGTTTGGTG CCAACTTAAACAGATACGC**ATG**GAAGATGCCAAAAACATTAAGAAGGGCCC
ΔBKRF3 uORFs	AAGCTTAGTCTGGCCTCCTTAAATTCACCTAAGAATGGGAGCAACCAGCTGGTCATCAGCCGCTGCGC AAACGGACTCAACGTGGTCTCCTTCTTTATCTCCATCCCGAAGCGAAGCAGCTCCGCCCTCACGAGCC ATCTCCGTGAGTTGTTAACCACCCCGGAGTCTCTTTACGGTTCATTCTCAGTGGAAGACCTGTTTGGTG CCAACTTAAACAGATACGC**ATG**GAAGATGCCAAAAACATTAAGAAGGGCCC
BORF2 uORF	AAGCTTACATATAGAGGAGCTAACCTTCGGGGCGGTTGCCTGTCTGGGGACATTTAGTGCTACTGACG GTTGGAGGAGGTCTGCCTTCAATTACCGTGGCTCTAGCCTCCCCGTGGTGGAGATTGACAGCTTTTAT TCCAACGTCTCTGACTGGGAGGTGATTCTCTAGACTTAACGGGAGGAAACAGGAGGAGGAGGGGGAC AAGAGCACAAAAGTGGTTCAGTGGACACCCACCACACAGC**ATG**GAAGATGCCAAAAACATTAAGAAGG GCCC
ΔBORF uORF	AAGCTTACATATAGAGGAGCTAACCTTCGGGGCGGTTGCCTGTCTGGGGACATTTAGTGCTACTGACG GTTGGAGGAGGTCTGCCTTCAATTACCGTGGCTCTAGCCTCCCCGTGGCGGAGATTGACAGCTTTTAT TCCAACGTCTCTGACTGGGAGGTGATTCTCTAGACTTAACGGGAGGAAACAGGAGGAGGAGGGGGAC AAGAGCACAAAAGTGGTTCAGTGGACACCCACCACACAGC**ATG**GAAGATGCCAAAAACATTAAGAAGG GCCC
wt EBNA3A TLS	GAGCTCGTTTAGTGAACCGTCAGATCACTAGAAGCTTAGATCAGATGGCATAGAGACAAGGACACCGA AGACCCCCAGAGCCCTCATCGCAGGGTTCTTACCATGTGGCCATGTAGGCCCACTTAACACTACAAGA CCTACGCCTCCCCATTCATCATGTAACCCGCAAATCATCTAAACCGACTGAAGAAACAGCCTCCTGCAC GTGAGCATAAGCTTCCACTACGGCCACGTCCCCGGCCTCCCGCTCGGTCTCTTAGAGAGTGGCTGCTA CGCATGAGAGCCAGCTTTGAGCCACCCACAGTAACCACCCAGCGCCAATCTGTCTACATAGAAGAAGA GGAGGATGAAGACTAAGTCACAGGCTTAGCCAGGTAACTTAGGAAGCGTTTCTTGAGCTTCCCTGGGA TGAGCGTTTGGGAGAGCTGATTCTGCAGCCCAGAGAGTAGTCTCAGGGCATCCTCTGGAGCCTGACC TGTGACCGTCGCATCATAGACCGCCAGTAGACCTGGGAGCAGATTCACCGCCGCGGCCGTCTCCTTTA AGACAAA**ATG**GAAGATGCCAAAAACATTAAGAAGGGCCC
ΔY2uORF EBNA3A TLS	GAGCTCGTTTAGTGAACCGTCAGATCACTAGAAGCTTAGATCAGATGGCATAGAGACAAGGACACCGA AGACCCCCAGAGCCCTCATCGCAGGGTTCTTACCATGTGGCCATGTAGGCCCACTTAACACTACAAGA CCTACGCCTCCCCATTCATCATGTAACCCGCAAATCATCTAAACCGACTGAAGAAACAGCCTCCTGCAC GTGAGCATAAGCTTCCACTACGGCCACGTCCCCGGCCTCCCGCTCGGTCTCTTAGAGAGTGGCTGCTA CGCATGAGAGCCAGCTTTGAGCCACCCACAGTAACCACCCAGCGCCAATCTGTCTACATAGAAGAAGA GGAGGACGAAGACTAAGTCACAGGCTTAGCCAGGTAACTTAGGAAGCGTTTCTTGAGCTTCCCTGGGA TGAGCGTTTGGGAGAGCTGATTCTGCAGCCCAGAGAGTAGTCTCAGGGCATCCTCTGGAGCCTGACC TGTGACCGTCGCATCATAGACCGCCAGTAGACCTGGGAGCAGATTCACCGCCGCGGCCGTCTCCTTTA AGACAAA**ATG**GAAGATGCCAAAAACATTAAGAAGGGCCC
ΔUuORF EBNA3A TLS	GAGCTCGTTTAGTGAACCGTCAGATCACTAGAAGCTTAGATCAGATGGCATAGAGACAAGGACACCGA AGACCCCCAGAGCCCTCATCGCAGGGTTCTTACCATGTGGCCATGTAGGCCCACTTAACACTACAAGA CCTACGCCTCCCCATTCATCATGTAACCCGCAAATCATCTAAACCGACTGAAGAAACAGCCTCCTGCAC GTGAGCATAAGCTTCCACTACGGCCACGTCCCCGGCCTCCCGCTCGGTCTCTTAGAGAGTGGCTGCTA CGCATGAGAGCCAGCTTTGAGCCACCCACAGTAACCACCCAGCGCCAATCTGTCTACATAGAAGAAGA GGAGGATGAAGACTAAGTCACAGGCTTAGCCAGGTAACTTAGGAAGCGTTTCTTGAGCTTCCCTGGGA CGAGCGTTTGGGAGAGCTGATTCTGCAGCCCAGAGAGTAGTCTCAGGGCATCCTCTGGAGCCTGACC TGTGACCGTCGCATCATAGACCGCCAGTAGACCTGGGAGCAGATTCACCGCCGCGGCCGTCTCCTTTA AGACAAA**ATG**GAAGATGCCAAAAACATTAAGAAGGGCCC
ΔY2/UuORF EBNA3A TLS	GAGCTCGTTTAGTGAACCGTCAGATCACTAGAAGCTTAGATCAGATGGCATAGAGACAAGGACACCGA AGACCCCCAGAGCCCTCATCGCAGGGTTCTTACCATGTGGCCATGTAGGCCCACTTAACACTACAAGA CCTACGCCTCCCCATTCATCATGTAACCCGCAAATCATCTAAACCGACTGAAGAAACAGCCTCCTGCAC GTGAGCATAAGCTTCCACTACGGCCACGTCCCCGGCCTCCCGCTCGGTCTCTTAGAGAGTGGCTGCTA CGCATGAGAGCCAGCTTTGAGCCACCCACAGTAACCACCCAGCGCCAATCTGTCTACATAGAAGAAGA GGAGGACGAAGACTAAGTCACAGGCTTAGCCAGGTAACTTAGGAAGCGTTTCTTGAGCTTCCCTGGGA CGAGCGTTTGGGAGAGCTGATTCTGCAGCCCAGAGAGTAGTCTCAGGGCATCCTCTGGAGCCTGACC TGTGACCGTCGCATCATAGACCGCCAGTAGACCTGGGAGCAGATTCACCGCCGCGGCCGTCTCCTTTA AGACAAA**ATG**GAAGATGCCAAAAACATTAAGAAGGGCCC
ΔuAUGs EBNA3A TLS	GAGCTCGTTTAGTGAACCGTCAGATCACTAGAAGCTTAGATCAGACGGCATAGAGACAAGGACACCGA AGACCCCCAGAGCCCTCATCGCAGGGTTCTTACCATGTGGCCACGTAGGCCCACTTAACACTACAAGA CCTACGCCTCCCCATTCATCACGTAACCCGCAAATCATCTAAACCGACTGAAGAAACAGCCTCCTGCAC GTGAGCATAAGCTTCCACTACGGCCACGTCCCCGGCCTCCCGCTCGGTCTCTTAGAGAGTGGCTGCTA CGCATGAGAGCCAGCTTTGAGCCACCCACAGTAACCACCCAGCGCCAATCTGTCTACATAGAAGAAGA GGAGGATGAAGACTAAGTCACAGGCTTAGCCAGGTAACTTAGGAAGCGTTTCTTGAGCTTCCCTGGGA TGAGCGTTTGGGAGAGCTGATTCTGCAGCCCAGAGAGTAGTCTCAGGGCATCCTCTGGAGCCTGACC TGTGACCGTCGCATCATAGACCGCCAGTAGACCTGGGAGCAGATTCACCGCCGCGGCCGTCTCCTTTA AGACAAA**ATG**GAAGATGCCAAAAACATTAAGAAGGGCCC
Δall uORFs EBNA3A TLS	GAGCTCGTTTAGTGAACCGTCAGATCACTAGAAGCTTAGATCAGACGGCATAGAGACAAGGACACCGA AGACCCCCAGAGCCCTCATCGCAGGGTTCTTACCATGTGGCCACGTAGGCCCACTTAACACTACAAGA CCTACGCCTCCCCATTCATCACGTAACCCGCAAATCATCTAAACCGACTGAAGAAACAGCCTCCTGCAC GTGAGCATAAGCTTCCACTACGGCCACGTCCCCGGCCTCCCGCTCGGTCTCTTAGAGAGTGGCTGCTA CGCATGAGAGCCAGCTTTGAGCCACCCACAGTAACCACCCAGCGCCAATCTGTCTACATAGAAGAAGA GGAGGACGAAGACTAAGTCACAGGCTTAGCCAGGTAACTTAGGAAGCGTTTCTTGAGCTTCCCTGGGA CGAGCGTTTGGGAGAGCTGATTCTGCAGCCCAGAGAGTAGTCTCAGGGCATCCTCTGGAGCCTGACC TGTGACCGTCGCATCATAGACCGCCAGTAGACCTGGGAGCAGATTCACCGCCGCGGCCGTCTCCTTTA AGACAAA**ATG**GAAGATGCCAAAAACATTAAGAAGGGCCC

Supplementary Table 6: Oligonucleotides used to clone the HA-tagged constructs.

target gene		primer sequence
wt TLS LMP1-HA	fwd	5'-ATATAAGCTTGCCTCCATCCCCAGAAACACG-3'
	rev	5'-TAGAATTCTAAGCGTAATCTGGCACATCGTATGGGTATCCTCCACCTCCTCCGTCATAGTAGCTTAGCTGAACTGGGC-3'
ΔuORF TLS LMP1-HA	fwd	5'-ATATAAGCTTGCCTCCATCCCCAGAAACACGCGTTGCTCTCTCGTAGGCGGCCTACATAAGCCTCTGTCACTGCTCCGTCAGCTTCTTTCCTCAGTTGCC-3'
wt TLS BORF2-HA	fwd	5'-ATATAAGCTTGCCTGTCTGGGGACATTTAGTGC-3'
	rev	5'-TAGAATTCTAAGCGTAATCTGGCACATCGTATGGGTATCCTCCACCTCCTCCTTGGCAAGATTCACAGGCTCGTTC-3'
ΔuORF TLS BORF2-HA	fwd	5'-ATATAAGCTTGCCTGTCTGGGGACATTTAGTGCTACTGACGGTTGGAGGAGGTCTGCCTTCAATTACCGTGGCTCTAGCCTCCCCGTGGCGGAGATTGACAGCTTTTATTCCAACG-3'
wt TLS BKRF3-HA	fwd	5'-ATAGGATCCTAAGAATGGGAGCAACCAGC-3'
	rev	5'-TAGGATCCTAAGCGTAATCTGGCACATCGTATGGGTATCCTCCACCTCCTCCCAGCCTCCAATCTATCTCACCGAG-3'
ΔuORF TLS BKRF3-HA	fwd	5'-ATAGGATCCAACAGATACGCATGGCATCGC-3'